9TH INTERNATIONAL SYMPOSIUM ON PARTICLE IMAGE VELOCIMETRY – PIV'11
Kobe, Japan, July 21-23, 2011

SAND2011-3567C

POD Analysis of the In-Cylinder Flow and Fuel Mole-fraction in a Hydrogen-Fueled Internal Combustion Engine

V.M. Salazar[1], S.A. Kaiser[2]

[1]Sandia National Laboratories, Livermore CA, USA
vmsalaz@sandia.gov

[2]University of Duisburg-Essen, Duisburg, Germany
sebastian.kaiser@uni-due.de

ABSTRACT

This work applies proper orthogonal decomposition (POD) to two-dimensional fields of velocity and fuel mole-fraction in the cylinder of an optically accessible internal combustion engine. The engine is fueled by direct injection of gaseous hydrogen during the compression stroke, which imparts strong convection and fuel inhomogeneity on the cylinder charge. Velocity and fuel-mole fraction in the vertical symmetry plane of the cylinder were acquired previously by two-component PIV and planar laser-induced fluorescence (PLIF), respectively. POD was performed to learn about the nature of cycle-to-cycle variability of flow and fuel distribution, which is expected to influence combustion and hence cyclic variability in engine performance.

The results indicate that the level of "organization" of the large-scale structure, characterized by the energy content in the low-order POD modes, changes throughout compression. The velocity field is not only less organized than fuel mole-fraction, but also its organization decreases as the piston approaches top dead center (TDC). Further analysis of the large-scale structure fluctuations, which characterize the cycle-to-cycle variations, showed that they are linked to the organization of the flow. For the fuel mole-fraction, because of the high level of organization, the cycle-to-cycle variability is small. In contrast, the flow field, which has less organization, also has greater cycle-to-cycle variability. Shortly before TDC, the fluctuations of the POD's first reconstruction coefficient are approximately four times higher for velocity than they are for fuel mole-fraction. The asymmetry between velocity and scalar may imply that for this engine configuration cyclic variation of combustion and engine performance could be dominated by velocity fluctuations.

1. INTRODUCTION

Energy security and environmental concerns are demanding cleaner and more efficient engines for automotive applications. With near-zero emissions and potential for high efficiency, hydrogen-fueled internal combustion engines (H2ICE) are a promising option [1]. Recent studies also show that vehicles powered by advanced H2ICEs can outperform today's gasoline and diesel vehicles and are competitive with those powered by fuel cells [2]. A key technology of advanced H2ICEs is direct injection (DI) of the hydrogen fuel into the cylinder, which offers flexibility for controlling emissions and optimizing engine efficiency. Several studies in DI-H2ICEs show that the extent of the benefits from DI depends greatly on the injection strategy and the details of the subsequent mixture formation process [3]. Therefore, understanding the details of in-cylinder turbulence, fuel-air mixing, and the cycle-to-cycle variability is an imperative step to improve the efficiency of future hydrogen engines.

Proper orthogonal decomposition (POD), a technique introduced to fluid dynamics by Lumley in 1967 [4], has shown the ability to objectively extract the dominant structures in a turbulent flow. In engines, POD has been applied to velocity measurements by particle image velocimetry (PIV) to gain fundamental insight into cycle-to-cycle variability and other in-cylinder phenomena. One of the first applications to in-cylinder flows was performed by Raposo *et al.* [5], who studied the dynamic behavior of coherent structures in velocity fields in a water-analogue test-rig. More recently, POD has been used to analyze velocity fields in optically-accessible gasoline and Diesel engines under motored conditions [6, 7]. Other engine-related applications include the application of POD to both computational fluid dynamics (CFD) and PIV data to analyze in-cylinder turbulence and to build low-dimensional models [6, 8].

Although POD has been applied mainly to velocity fields, in principle the technique could be used on any other measured variable with spatio-temporal fluctuations. For example, Palacios *et al.* [9] applied POD to video data of flames in a premixed burner, identifying the dominant spatial structures and their temporal evolution. Applications of POD to engine combustion have also been reported. In 2007, Bizon *et al.* [10] used POD to interpolate data between two consecutive flame images recorded in an optically-accessible spark ignited engine. Later the same authors [11] applied POD to cycle-resolved image series of combustion in gasoline and Diesel engines in order to investigate cycle-to-cycle variability. Such analysis required the decomposition of the images into mean, coherent, and incoherent parts. The results showed that the low-order POD modes give an indication of the cycle-to-cycle variations. Besides combustion, POD has also been used to analyze simultaneously recorded data of fuel mole-fraction and velocity in order to identify misfires in a GDI engine [12].

This paper reports the application of POD to separately acquired quantitative measurements of velocity and fuel mole-fraction in a spark-ignited H2ICE. The main goal is to gain insight into cycle-to-cycle fluctuations and their influence on fuel-air mixing.

2. PROPER ORTHOGONAL DECOMPOSITION (POD).

A detailed description of application of POD to turbulent flows is out of the scope of this paper. The book of Holmes *et al.* [13] presents a complete review of the technique. Nevertheless, for completeness a brief description of how POD was applied to images of velocity and fuel mole-fraction is provided.

Application of classical POD, as introduced by Lumley [4, 13], is computationally expensive, especially when the number of grid points greatly exceeds the number of measured fields. To overcome this issue, Sirovich [14] introduced the "method of snapshots", which is computationally more affordable and is the one adopted in this paper. In snapshot POD, each instantaneous PIV field U^k is considered as a snapshot, where the index k runs through the K phase-locked measurements that comprise the PIV data set. In two dimensions, U^k has two velocity components, u and v, with M grid points each, making a total of $2 \times M$ velocity data points per snapshot. To perform the POD, the snapshots are arranged as follows [15]:

$$U = \begin{bmatrix} u_1^1 & \cdots & u_1^K \\ \vdots & \vdots & \vdots \\ u_M^1 & \cdots & u_M^K \\ v_1^1 & \cdots & v_1^K \\ \vdots & \vdots & \vdots \\ v_M^1 & \cdots & v_M^K \end{bmatrix} \quad (1)$$

where the *kth* column corresponds to the *kth* snapshot. The next step is to solve the eigenvalue problem:

$$CA = \lambda A \quad (2)$$

where A is the eigenvector matrix, λ the corresponding eigenvalues and C the velocity-time correlation matrix defined as:

$$C = U^T U \quad (3)$$

where the superscript T denotes transpose. In **Equation 2**, the columns of A represent the new basis from which we construct the POD modes. Furthermore, for a given velocity data set, the eigenvalues λ^k are an indicator of the fraction of energy contained in each POD mode [14]. Therefore, it is convenient to rank them according to their magnitude i.e.: $\lambda^1 > \lambda^2 > ... > \lambda^K$. The relative energy content of each mode is obtained by normalizing the eigenvalues:

$$\varepsilon = \frac{\lambda^k}{\sum_{k=1}^{K} \lambda^k} \quad (4)$$

Then, each *kth* POD mode ψ^k is constructed from its eigenvector A^k as follows:

$$\psi^k = \frac{UA^k}{\left\| UA^k \right\|}, \text{ with } k = 1,2, ..., K \quad (5)$$

Finally, each original velocity data field can be reconstructed from the POD modes in the following manner:

$$U^k = \sum_{j=1}^{K} a_j^k \psi^j \quad (6)$$

where the coefficients a_j^k, are the projection of the U^k velocity field onto the ψ^j mode:

$$a_j^k = (\psi^j)^T U^k \quad (7)$$

Although the description provided above is focused on the velocity data sets, the same algorithm was applied to the scalar field of fuel mole-fraction.

3. EXPERIMENTAL DATA

The measurements of velocity and fuel mole-fraction used for the present analysis have been reported in previous publications [16, 17]. Therefore only a brief overview of the experimental arrangement and the operating conditions will be provided. The experiments were performed using a passenger-car sized, optically accessible, single-cylinder engine, shown schematically in **Figure 1a**. This four-stroke engine has a flat-top piston and a four-valve head with a pent-roof combustion chamber. With the engine motored at 1500 RPM, hydrogen was supplied at 100 bar directly into the combustion chamber by an angled single-hole nozzle shown in **Figure 1b**. The injection, which lasted for 17.5 °CA and started just after intake valve closure (-140 °CA[1]), resulted in a global equivalence-ratio of 0.25 (or a hydrogen mole-fraction of 0.095).

Planar laser induced fluorescence (PLIF) of gaseous acetone [16] and particle image velocimetry (PIV) [17] were used to measure fuel mole-fraction and flow field, respectively. These measurements were performed in the vertical symmetry plane (**Figure 1a and c**) from BDC to near TDC. Two intake-flow configurations were tested: low tumble with a tumble ratio of 0.22, corresponding to unmodified intake ports, and high tumble with a tumble ratio of 0.70, resulting from intake modification. However, for brevity only data from the high-tumble case will be analyzed in this paper.

[1] The crank-angle convention used here assigns 0 °CA to TDC, i.e. crank angles throughout the compression stroke are negative.

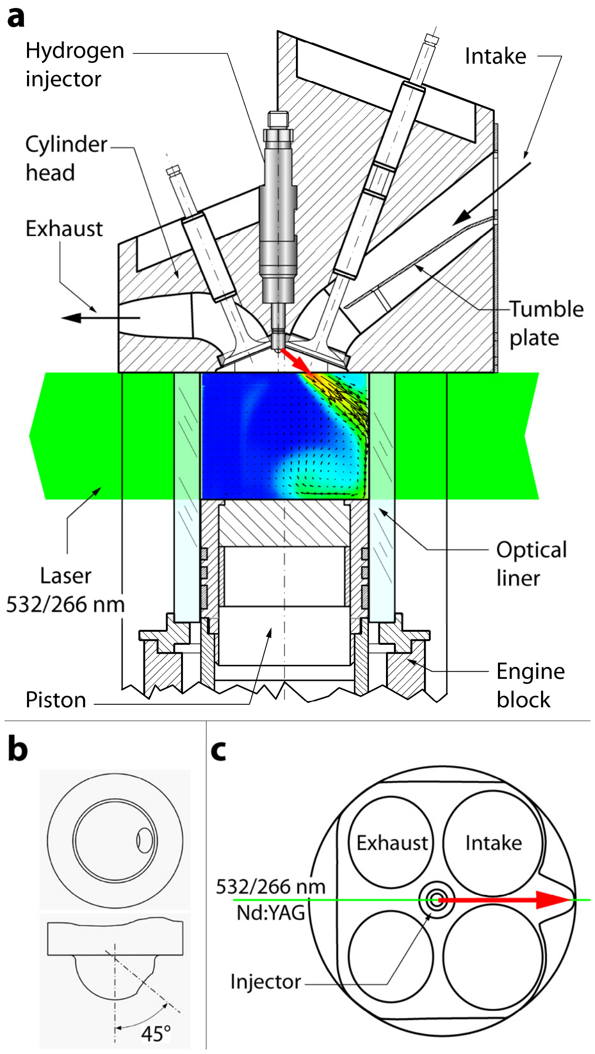

Figure 1. Schematic of the optically-accessible engine. (**a**) Upper portion of the engine with the measurement plane, (**b**) Geometry of the single-hole injector nozzle location and (**c**), targeting of injector with respect to the combustion chamber.

3. RESULTS

POD was performed for all data sets of velocity and fuel mole-fraction from [16, 17], i.e. for a series of crank angles during the compression stroke. For an initial overview of the morphology of the different POD modes, we first focus on results at -55 °CA. The ensemble mean and the first POD modes are shown in **Figure 2.** In both velocity and fuel mole-fraction, the first POD mode is almost identical to the mean. However, the remaining POD modes show morphologies that vary greatly from each other.

For velocity, each normalized eigenvalue of the POD represents the relative energy content of the associated POD mode. In contrast, for fuel mole-fraction, the eigenvalues do not have an obvious physical meaning. Nevertheless, the eigenvalues still correspond to the contribution of each POD mode to the fuel-mole fraction reconstruction. The cumulative normalized eigenvalues for velocity and fuel mole-fraction are shown in **Figure 3**. They clearly indicate that to reconstruct a typical fuel mole-fraction image only few modes are required. However, in the case of velocity, a relatively large number of modes are needed. For example, to reach the 95% of the cumulative normalized eigenvalues, only 4% of the fuel mole-fraction modes are required, compared to almost 70% for velocity. Although not presented here, the situation is similar at other crank angles.

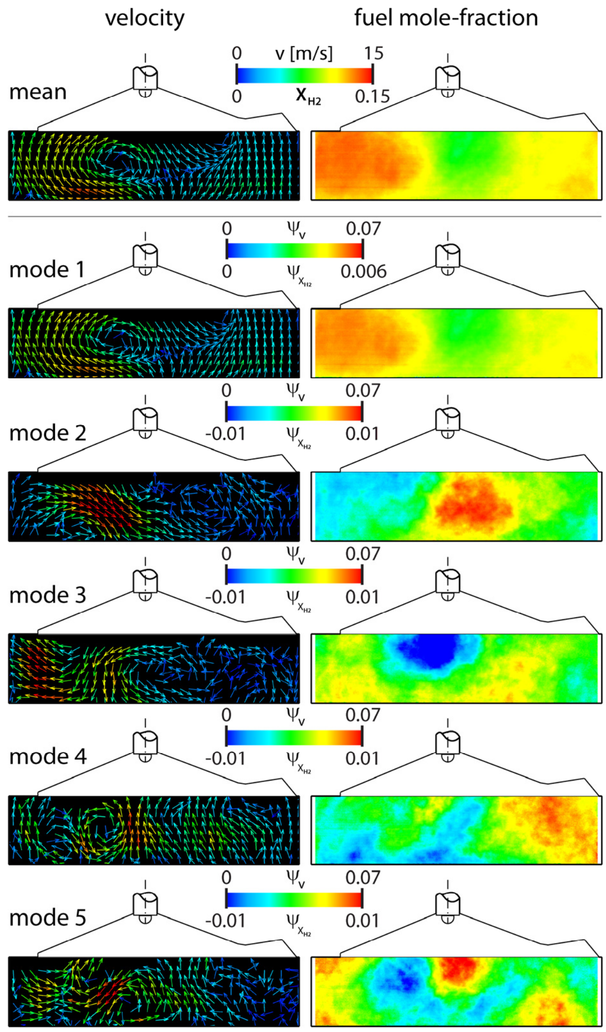

Figure 2. (Top row) Ensemble-average velocity and hydrogen molar fraction at -55°CA. (Second to sixth rows) First five POD modes for velocity (PIV) and fuel mole-fraction (PLIF).

The relative energy content in the POD modes also provides information about the cycle-to-cycle variability and the morphology of the flow. Liu and Haworth [8] showed that flows that need only few POD modes to reach a high fraction of the total energy are very organized. These authors [8] also illustrated that as consequence of this high organization, the flows had low cycle-to-cycle variability. Conversely, a flow that requires many modes to reach the same fractional energy content is not well organized and has higher cycle-to-cycle variability. A limiting case would be a data set where all snap shots are identical. In such a hypothetical case, all the energy would be concentrated in the first mode and it would not exhibit any cycle-to-cycle variability. Applying this interpretation to the fuel mole-fraction fields, **Figure 3** indicates that the fuel mole-fraction is very organized and therefore more repeatable. The velocity field, on the other hand, is less organized and thus is expected to exhibit higher cycle-to-cycle variability.

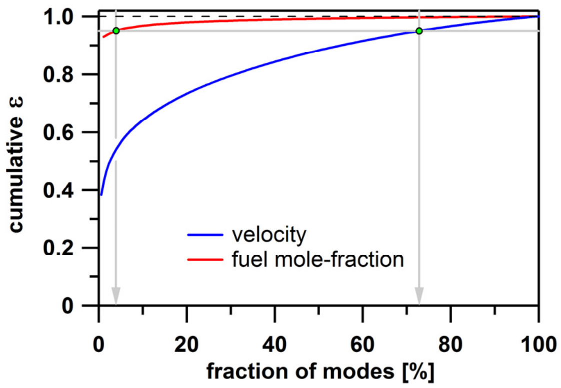

Figure 3. Cumulative normalized eigenvalues as a function of the fraction of the total number of modes for velocity and fuel mole-fraction at -55°CA.

After this first look at the PODs at a representative crank angle, we now expand the analysis to the whole compression stroke after injection. **Figure 4** shows that the relative contribution of the first POD modes, and therefore the organization, changes throughout compression. The fuel distribution is very organized during the injection process (ending at -120 °CA), which indicates that it is very repeatable with low cycle-to-cycle variability. Turbulent fluctuations within the injection jet may only be marginally resolved here. However, after injection, the level of organization decreases and reaches its lowest value at about -100 °CA. During the remaining part of compression, the organization level increases and at ignition time (around -30°CA) the fuel distribution shows even a higher level of organization than during injection.

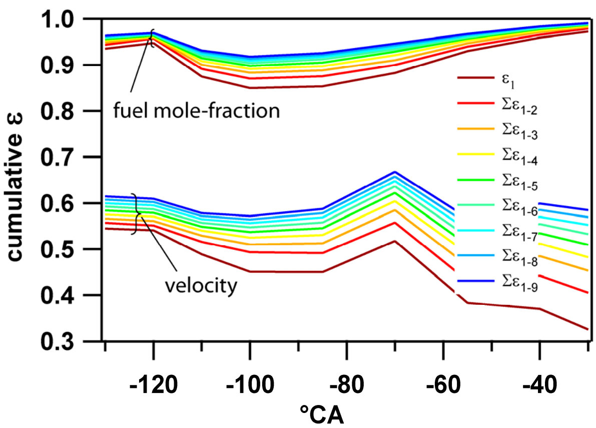

Figure 4. Cumulative normalized eigenvalues for velocity and fuel mole-fraction throughout compression.

For the velocity, the cumulative energy contribution behaves qualitatively different. The relative contribution of the first modes is always less than for the fuel mole-fraction. Also for velocity the contribution of the first modes decreases after the end of injection, but in this case, after peaking at mid-compression it decreases as the piston approaches TDC. The fact that the flow becomes less organized near TDC indicates that the flow is less stable from cycle-to-cycle, which may compromise the cycle-to-cycle variability of the combustion process. However, the implications of the difference between velocity and fuel mole-fraction on combustion will depend on which of these variables has greater influence on flame propagation.

To further investigate the cycle-to-cycle variability, the single shots were decomposed into mean, coherent and fluctuating components [11, 18]. The mean field, which represents the large scale flow structures [11, 18], was computed by adding the first *m* POD modes as in **Equation 6**. To determine how many *m* POD modes were necessary to capture the "mean", the reconstructed mean field was correlated with the mean obtained by ensemble averaging the instantaneous fields. Typically, only the first mode was needed to obtain the highest correlation. Therefore, the first POD mode and its corresponding coefficient a_1 can be used to represent the large flow structure in each cycle.

In engines, the fluctuations of the POD's mean component are typically attributed to the cycle-to-cycle fluctuations in the large-scale flow [18]. Therefore the first mode and its coefficients were used to gain further insight of the cycle-to-cycle fluctuations [11, 18]. **Figure 5** shows the variability of the first POD coefficient characterized by its coefficient of variance (COV), defined as the standard deviation divided by the mean.

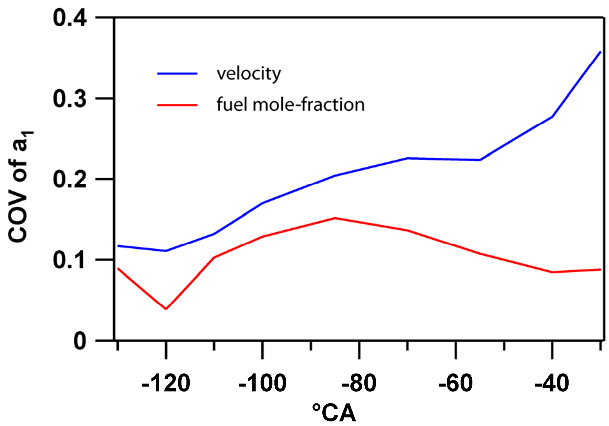

Figure 5. COV of the first POD coefficient a_1 for velocity and fuel mole-fraction throughout compression.

The results in **Figure 5** confirm some of the implications of **Figure 4**, i.e. the fuel mole-fraction has much less cyclic fluctuations than the velocity field. Also, while the cycle-to-cycle variability of the velocity increases as the piston approaches TDC, for the fuel mole-fraction the variability increases only until the middle of the compression stroke, but then decreases, reaching a value that is approximately four times smaller than for the velocity. This again implies that cycle-to-cycle variations in combustion, which result in such observables as COV of IMEP, may be more influenced by fluctuations in the flow field than in fuel mole-fraction. Direct confirmation of this speculation would necessitate cycle-correlated measurements of engine performance and pre-combustion flow and fuel distribution.

4. CONCLUSIONS

POD was applied to velocity and fuel mole-fraction measured in an optically-accessible engine fueled by direct injection of hydrogen. The POD analysis allowed insight into the organization and cycle-to-cycle fluctuations of velocity and fuel mole-fraction. The main findings of this study can be summarized as follows:

- The organization of the fuel distribution and flow field change throughout the compression process. The fuel mole-fraction appears to be highly organized during injection and near TDC. The flow field, on the other hand, not only starts out less organized than the fuel distribution, but also shows further degradation in organization as the piston approaches TDC. This may indicate that in the current engine configuration the velocity field has greater influence on cyclic variability of engine performance than the fuel mole-fraction has.

- Statistical analysis of the first POD coefficient a_1 shows that the cycle-to-cycle fluctuations of the fuel mole-fraction are relatively constant with a COV below 10%. The cycle-to-cycle variability in the velocity data is significantly higher at all crank angles, reaching a COV of approximately 40% near TDC.

ACKNOWLEDGMENTS

The excellent technical support by G. Hux is greatly appreciated. Financial support for this research was provided by the U.S. Department of Energy, Office of Energy Efficiency and Renewable Energy, program manager Gurpreet Singh. The research was performed at the Combustion Research Facility, Sandia National Laboratories, Livermore, California. Sandia is operated by Sandia Corporation, a Lockheed Martin Company, for the United States Department of Energy's National Nuclear Security Administration under contract DE-AC04-94AL85000.

REFERENCES

[1] White, C.M., Steeper, R.R., and Lutz, A.E., (2006) The Hydrogen-Fueled Internal Combustion Engine: A Technical Review. *Int. J. Hydrogen Energy* **21(10)**, 1292-1305.

[2] Rousseau, A., Wallner, T., Sylvain, T., and Lohse-Busch, H., (2008) Prospects on Fuel Economy Improvements for Hydrogen Powered Vehicles. *SAE Technical Paper* 2008-01-2378.

[3] Wallner, T., Nande, A.M., and Naber, J.D., (2009) Study of Basic Injection Configurations using a Direct-Injection Hydrogen Research Engine. *SAE Int. J. Engines* **2(1)**, 1221-1230.

[4] Lumley, J.L., (1967) The Structure of Inhomogeneous Turbulent Flows. *Atmospheric Turbulence and Radio Wave Propagation*, ed. by Yaglom, A.M., and Tatarski, V.I. (Nauka, Moscow) pp. 166-178.

[5] Raposo, J., Hentschel, W., and Merzkirch, W., (2000) Analysis of the Dynamical Behaviour of Coherent Structures in In-Cylinder Flows of Internal Combustion Engines. *Proc. 10th Int. Symp. on Applications of Laser Techniques to Fluid Mechanics*, July 10-13, 2000.

[6] Keromnes, A., Dujol, C., and Guibert, P., (2010) Aerodynamic Control Inside an Internal Combustion Engine. *Meas. Sci. Tech.* **21**(2010) 125404.

[7] Kapitza, L., Imberdis, O., Bensler, H.P., Willand, J., and Thevenin, D., (2010) An Experimental Analysis of the Turbulent Structures Generated by the Intake Port of a DISI-Engine. *Exp. Fluids* **48**(2010), 265-280.

[8] Liu, K., and Haworth, D., (2011) Development and Assessment of POD for Analysis of Turbulent Flow in Piston Engines. *SAE Technical Paper* 2011-01-0830.

[9] Palacios, A., Armbruster, D, Kostelich, E.J., Stone, E., (1996) Analysing the Dynamics of Cellular Flames. *Physica D* **96**(1996), 132-161.

[10] Bizon, K., Continillo, G., Merola, S.S., and Vaglieco, B.M, (2007) Application of Proper Orthogonal Decomposition to the Analysis of I.C.E. Space and Time Resolved Data. *SAE Technical Paper* 2007-24-0007.

[11] Bizon, K., Continillo, G., Mancaruso, E., Merola, S.S., and Vaglieco, B.M, (2010) POD-based Analysis of Combustion Images in Optically Accessible Engines. *Combustion and Flame* **157**(2010), 632-640.

[12] Chen, H., Reuss, D.L., and Sick, V., (2011) Analysis of Misfires in a Direct Injection Engine Using Proper-Orthogonal Decomposition. *Proc. 7th US National Combustion Meeting*, Atlanta, GA. March 20-23, 2011.

[13] Holmes, P., Lumley, J.L., and Berkooz, G., (1996) Turbulence, Coherent Structures, Dynamical Systems and Symmetry. *Cambridge University Press.*

[14] Sirovich, L., (1987) Turbulence and the Dynamics of Coherent Structures. *Quarterly of Applied Mathematics* **45** (1987), 561-590.

[15] Meyer, K.E., Cavar, D., and Pedersen, J.M., (2007) POD as Tool for Comparison of PIV and LES Data. *Proc. 7th Int. Symp. Particle Image Velocimetry, Roma, Italy.* September 11-14, 2007.

[16] Salazar, V.M., and Kaiser, S.A., (2010) Influence of the In-Cylinder Flow Field (Tumble) on the Fuel Distribution in a DI Hydrogen Engine Using a Single-Hole Injector. *SAE Int. J. Engines* **3(1)**, 309-325.

[17] Salazar, V.M. and Kaiser, S.A., (2011) Interaction of Intake-Induced Flow and Injection Jet in a Direct-Injection Hydrogen-Fueled Engine Measure by PIV. *SAE Technical Paper* 2011-01-0673.

[18] Roudnitzky, S., Druault, P., Guibert, P., (2006) Proper Orthogonal Decomposition of In-Cylinder Engine Flow into Mean Component, Coherent Structures and Random Gaussian Fluctuations. *J. Turbulence* **7(70)**, 1-19.